Journal Pre-proof

Improved accuracy in pentraxin-3 quantification assisted by aqueous biphasic systems as serum pretreatment strategies

Maria S.M. Mendes, Marguerita E. Rosa, João A.P. Coutinho, Mara G. Freire, Francisca A. e Silva

PII: S0141-8130(23)04437-9

DOI: https://doi.org/10.1016/j.ijbiomac.2023.127540

Reference: BIOMAC 127540

To appear in: *International Journal of Biological Macromolecules*

Received date: 3 July 2023

Revised date: 15 October 2023

Accepted date: 17 October 2023

Please cite this article as: M.S.M. Mendes, M.E. Rosa, J.A.P. Coutinho, et al., Improved accuracy in pentraxin-3 quantification assisted by aqueous biphasic systems as serum pretreatment strategies, *International Journal of Biological Macromolecules* (2023), https://doi.org/10.1016/j.ijbiomac.2023.127540

Improved accuracy in pentraxin-3 quantification assisted by aqueous biphasic systems as serum pretreatment strategies

Maria S. M. Mendes[‡1], Marguerita E. Rosa[‡1], João A. P. Coutinho[1], Mara G. Freire[1*], Francisca A. e Silva[1*]

[1] CICECO - Aveiro Institute of Materials, Department of Chemistry, University of Aveiro, Aveiro, Portugal

[‡] Maria S. M. Mendes and Marguerita E. Rosa contributed equally to this work.

*To whom correspondence may be addressed E-mail: maragfreire@ua.pt; francisca.silva@ua.pt

Abstract

Although pentraxin-3 holds promise as a diagnosis/prognosis biomarker of microbial infections and lung cancer, its analysis in human serum can be constrained by matrix effects caused by high abundance proteins – human serum albumin and immunoglobulin G. Aqueous biphasic systems composed of polymers and citrate buffer are here proposed as a serum pretreatment step to improve the accuracy of pentraxin-3 analysis. Binodal curves were determined to identify the compositions required to form ABS and to correlate the polymers' properties and performance in serum pretreatment and biomarker extraction. Aqueous biphasic systems were evaluated regarding their ability to deplete human serum albumin and immunoglobulin G at the interphase. Polymers of relatively high to intermediate hydrophobicity were unveiled as efficient components to deplete high abundance serum proteins. Considering the possibility to extract pentraxin-3 from human serum into the polymer-rich phase, the system composed of polyethylene glycol with a molecular weight of 1000 $g \cdot mol^{-1}$ simultaneously achieved >93% of human serum albumin and immunoglobulin G depletion and complete biomarker extraction. The accuracy of analysis of pretreated human serum by enzyme-linked immunosorbent assays outperformed that of a non-pretreated sample, with a relative error of 0.8% compared to 14.6%, contributing to boost pentraxin-3 usefulness as a biomarker.

Keywords

Pentraxin-3, Human serum, Sample pretreatment, Aqueous biphasic system, Three-phase partitioning systems.

1. Introduction

Pentraxin-3 (PTX-3) is a 45 KDa glycoprotein that belongs to the pentraxin family. This family is arranged into two sub-groups, the short and the long pentraxins, with PTX-3 falling within the latter category. PTX-3 composition comprises 381 amino acids, each composed of a signal peptide (residues 1-17), a N-terminal domain (residues 18-178) and a C-terminal do-main (residues 179-381) connected through disulphide bonds [1]. The C-terminal domain is also called the "pentraxin domain" since it is a well-conserved sequence of around 202 amino acids across the pentraxin family [1,2]. Contrarily to short pentraxins that are only produced in the liver in response to interleukin-6 (IL-6), PTX-3 is produced by a variety of cell types, entailing monocytes, macrophages, fibroblasts, and epithelial cells. PTX-3 is produced as a response to several inflammatory or infectious events, especially intensified by interleukin-10 (IL-10) [3]. It can be thus considered a biomarker for innate immunity and inflammation as its blood levels rapidly raise from < 2 $ng \cdot mL^{-1}$ under normal conditions to 200-800 $ng \cdot mL^{-1}$ under inflammatory and infectious conditions (e.g., endotoxic shock and sepsis) [2–4]. In addition to the immune system activation, PTX-3 also takes a part in tumor progression by interposing within the PI3K/AKT/mTOR signaling pathway, essential for cell cycle regulation [2]. PTX-3 has been shown to induce tumor cell proliferation, apoptosis, and metastasis in several types of cancer, including lung cancer, head and neck squamous cell carcinoma and breast cancer [2]. Considering lung cancer, despite the limited predictive role, PTX-3 levels in serum correlated well with the presence versus the absence of the disease in high-risk populations comprising heavy smokers [5,6]. Its levels in serum are close to 1 $ng \cdot mL^{-1}$ in healthy individuals and close to 5 $ng \cdot mL^{-1}$ in lung cancer patients [7,8]. Moreover, the prognostic value of this glycoprotein is justified by the positive correlation between its levels in serum and tumor stage, disease aggressiveness, and survival in both small cell and non-small cell lung cancer patients [5,9,10].

PTX-3 can be present in blood-derived samples (including serum and plasma), the most clinically relevant body fluids, but also in urine, cerebrospinal, pleural and amniotic fluids [11]. To assess its concentration in biological samples, analytical methods such as surface plasmon resonance (SPR) [12] and enzyme-linked immunosorbent assay (ELISA) [10,11] have been used. Among these, ELISA is the preferred method to quantify PTX-3 since it features high accuracy and precision of analysis and lower limits of detection (LODs) than other analytical methods [13]. Despite its enhanced analytical performance, the accuracy of ELISA assays involving complex samples is still limited by background noises and non-specific reactions that may lead to false positive and negative results [14]. Accordingly, as for other biomarkers, the complex composition of the matrix is a major barrier to the accurate analysis of PTX-3 in serum and its further use in clinical settings. In serum proteome, human serum albumin (HSA) and immunoglobulin G (IgG) account for over 80% of the protein content (corresponding to the $mg \cdot mL^{-1}$ range), while the concentration of low abundance proteins such as PTX-3 commonly falls within the $ng \cdot mL^{-1}$ range [15]. The discrepancy between these orders of magnitude endows HSA and IgG with the capacity to interfere in the detection and quantification of PTX-3 [16].

To overcome these interferences, aqueous biphasic systems (ABS) are proposed in this work to be used as a sample pretreatment technique prior to PTX-3 analysis by ELISA. ABS belong to a class of liquid-liquid extraction systems that combine at least two incompatible solutes (e.g., two polymers, two salts or a polymer and a salt) in water as a replacement for water-immiscible organic solvents [17]. Because of the numerous combinations of ABS constituents available, a much wider tailoring ability is enabled, allowing to improve the performance/selectivity/cost-efficiency of sample pretreatment and biomarker extraction [18–20]. Additionally, it has been reported that upon the addition of complex samples in ABS, protein precipitation events can occur at the systems' interphase, leading to the formation of three-phase partitioning (TPP) systems [21,22]. This phenomenon arises from the differential partition/precipitation of proteins in ABS, i.e., between the top, inter or bottom phases and it is here used as the basis to design a human serum pretreatment step. We have recently overviewed the potential of ABS to support the analysis of disease biomarkers [23]. ABS can be used to prepare biological samples for proteomic studies assisting the identification/discovery of biomarkers [24], as extraction techniques supporting laboratory-reliant [25] and point-of-care analyses [26], and as confinement strategies within multiplex immunoassays [27]. Regarding the analysis of cancer biomarkers, successful applications of ABS have been reported with prostate-specific antigen (PSA) [20,28] and extracellular vesicles [29]; however, to the best of our knowledge, there are no previous reports regarding the improved analysis of PTX-3 by using ABS. To achieve our objective, the ternary phase diagrams of ABS composed of polymers, either homo or copolymers, and citrate buffer were initially determined to identify biphasic mixture compositions and to further allow establishing structure-properties-performance relationships in serum pretreatment and biomarker extraction. Then, adequate sample pretreatment systems were defined according to their aptitude to simultaneously deplete high abundance serum proteins at the interphase of the systems (here referred to as ABS-TPP) aptitude and extract PTX-3 in one of the ABS aqueous phases. The best performing ABS-TPP was further evaluated regarding its impact on the accuracy of PTX-3 quantification by ELISA as compared to non-pretreated serum. A layout of the new analytical approach here proposed is provided in Figure 1.

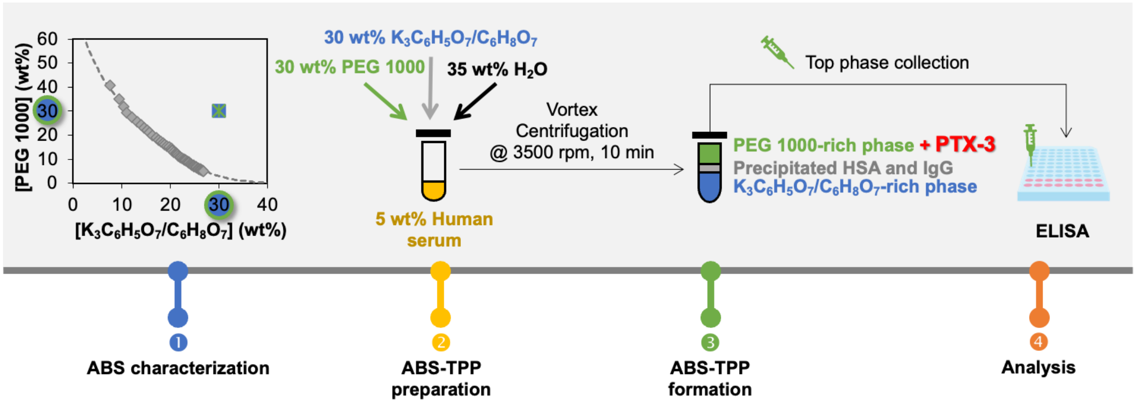

Figure 1. Experimental layout of the analytical method proposed to improve the analysis of PTX-3 by ELISA.

2. Materials and Methods

2.1 Materials

The ABS studied in this work were formed using homopolymers/copolymers and a citrate buffered salt. The homopolymers include polyethylene glycols (PEGs) of different molecular weights, namely 400, 600, 1000 and 2000 g·mol^{-1} (herein abbreviated as PEG 400, PEG 600, PEG 1000, and PEG 2000, respectively) and polypropylene glycol of average molecular weight 400 g·mol^{-1} (PPG 400). All polymers were acquired from Alfa Aesar, except PEG 400 and PPG 400 that were acquired from Sigma-Aldrich. The copolymers used included Pluronic PE6200 and PE6400 (PEG-block-PPG-block-PEG-block), both from BASF, as well as Pluronic L35 (PEG-block-PPG-block-PEG-block) and UCON (PEG-ran-PPG), both from Sigma-Aldrich. The chemical structures of the polymers are represented in Figure S1 in the Supplementary Information also including the polymers molecular weight (MW), arrangement and percentage of PEG (%PEG). For the citrate buffered salt preparation, potassium citrate tribasic monohydrate ($K_3C_6H_5O_7{\cdot}H_2O$, purity ≥ 99%) was obtained from Acros Organics and citric acid ($C_6H_8O_7{\cdot}H_2O$, purity ≥ 99.5%) from Panreac.

The human serum used was obtained from Sigma-Aldrich (H4522- Lot # SLBX6353) and kept at -20 °C up to use. For the preparation of the standards of the immunoglobulin G (IgG) and human serum albumin (HSA) calibration curves, a solution of purified human IgG (29.4 $mg{\cdot}mL^{-1}$) was obtained from Innovative researched, Inc. and a solution of HSA was prepared using a lyophilized powder of human albumin (purity ≥ 96%) purchased from Alfa Aesar. The quantification of pentraxin 3 (PTX-3) was performed using a commercially available enzyme- linked immunosorbent assay (ELISA) kit (ab214570), purchased from abcam and kept in storage at 4 °C. The ELISA kit included a pre-coated plate, capture/detection antibodies, buffers, diluents, substrates and lyophilized PTX-3 that was reconstituted by addition of a buffer to generate a stock solution with 10000 $pg{\cdot}mL^{-1}$. The stock solution was then used to prepare the standard solutions for the calibration curve, and the PTX-3 aqueous solution/spiked human serum for the extraction studies. For the Size-Exclusion High-Performance Liquid Chromatography (SE-HPLC) mobile phase, double distilled water, passed by a reverse osmosis system and further treated with a Milli-Q plus 185 water purification apparatus as well as the salts sodium di-hydrogen phosphate 1-hydrate, $NaH_2PO_4{\cdot}H_2O$ (99 wt% of purity) and di-sodium hydrogen phosphate 7-hydrate, $Na_2HPO_4{\cdot}7H_2O$ (99 wt% of purity), both from Panreac Applichem, were used. Phosphate buffered saline (PBS) 0,001M (pH 7.2-7.6) was prepared from Sigma-Aldrich (Lot # SLF6818), dissolving one tablet in 200 mL of distilled water.

2.2 Determination and characterization of ternary phase diagrams

Ternary phase diagrams for the systems composed of the homopolymers PPG 400, PEG 400, PEG 600, PEG 1000, and PEG 2000, or the copolymers Pluronic PE6200, PE6400, L35 and UCON and citrate buffer ($K_3C_6H_5O_7/C_6H_8O_7$) at pH ≈ 7 were characterized through the determination of the binodal curves and the tie-lines (TLs). The phase diagrams of PEG 400, PEG 600, PEG 1000 and PEG 2000 were already defined by Ferreira et al. [30] and are in agreement with the data reported. The binodal curve of each ABS was determined through the cloud point titration method at 25 (± 1) °C and atmospheric pressure (widely used and previously described by us) [30]. Aqueous solutions of $K_3C_6H_5O_7/C_6H_8O_7$ at pH ≈ 7 at circa 50 wt% and aqueous solutions of the different polymers/copolymers (with concentrations ranging from 30 wt% to 70 wt%) were used. Repeatedly and under continuous stirring, the drop-wise addition of the $K_3C_6H_5O_7/C_6H_8O_7$ aqueous solution to the homopolymer/copolymer solution was done until getting a cloudy solution (biphasic region) and was interspersed with the drop wise addition of water until a clear and limpid solution is met (monophasic region). The ternary system compositions after the addition of the salt solution or pure water were determined by weight quantification within an uncertainty of ± 10^{-4} g.

The tie-lines (TLs) of each phase diagram were determined by a gravimetric method described by Merchuk et al. [31] using mixture compositions where all systems are within the two-phase regime. The selected mixtures (30 wt% of homopolymer/copolymer + 30 wt% of $K_3C_6H_5O_7/C_6H_8O_7$ + 40 wt% of water) were prepared by weighing the proper quantity of each ABS component, i.e., homopolymer/copolymer, $K_3C_6H_5O_7/C_6H_8O_7$, and water. Then, each mixture was vigorously stirred, centrifuged for 10 min at 3500 rpm and left in equilibrium for more 10 min at 25 °C to ensure that the coexisting phases are in equilibrium. After separation of the two phases, each phase was carefully weighed within an uncertainty of ± 10^{-4} g and collected for pH measurements. The pH values of both the top phase (polymer-rich phase) and the bottom phase (salt-rich phase) were measured at 25 °C using a pH/Conductometer from Metrohm within an uncertainty of ± 0.02. To calibrate the pH meter two buffers, also from Metrohm, with pH values of 4.00 and 7.00 were used. The experimental points obtained to determine the binodal curve were correlated using the three-parameter equation proposed by Merchuk et al. [31] (Equation 1).

$$[Polymer] = A exp\ (B[Salt]^{0.5} - C[Salt]^{3}) \qquad (1)$$

where [Polymer] and [Salt] represent the weight percentage (wt%) of polymer/copolymer and salt, respectively, and *A*, *B*, and *C* correspond to the adjusted parameters obtained by least-squares regression. Each individual TL was determined by the application of the lever-arm rule to the relationship between the weight of the top phase and the overall system composition. For the determination of the TLs, the following system of four equation and four unknown variables (Equations 2 to 5) was used to calculate the concentration of homopolymer/copolymer and $K_3C_6H_5O_7/C_6H_8O_7$ in each phase ($[\text{Polymer}]_{\text{Top}}$, $[\text{Salt}]_{\text{Top}}$, $[\text{Polymer}]_{\text{Bottom}}$ and $[\text{Salt}]_{\text{Bottom}}$, respectively):

$$[Polymer]_{Top} = Aexp\,[\left(B[Salt]_{Top}^{0.5}\right) - \left(C[Salt]_{Top}^{3}\right)] \quad (2)$$

$$[Polymer]_{Bottom} = Aexp\,[\left(B[Salt]_{Bottom}^{0.5}\right) - \left(C[Salt]_{Bottom}^{3}\right)] \quad (3)$$

$$[Polymer]_{Top} = \frac{[Polymer]_M}{\alpha} - \left(\frac{1-\alpha}{\alpha}\right)[Polymer]_{Bottom} \quad (4)$$

$$[Salt]_{Top} = \frac{[Salt]_M}{\alpha} - \left(\frac{1-\alpha}{\alpha}\right)[Salt]_{Bottom} \quad (5)$$

where the subscripts "Top", "Bottom" and "M" represent the top phase, the bottom phase, and the mixture composition, respectively. The parameter α is the ratio between the top phase and the total weight of the mixture. For the calculation of each tie-line length (TLL), the Equation 6 was applied:

$$TLL = \sqrt{([Salt]_{Top} - [Salt]_{Bottom})^2 + ([Polymer]_{Top} - [Polymer]_{Bottom})^2}$$

(6)

2.3 Depletion of human serum albumin and immunoglobulin G

For the depletion studies, the mixture composition adopted was 30 wt% of homopolymer/copolymer, 30 wt% of $K_3C_6H_5O_7/C_6H_8O_7$, 5 wt% of human serum and 35 wt% of water. ABS were prepared by weighing the appropriate amount of each component, within ± 10^{-4} g, and mixing until all components were dissolved. Each mixture was stirred, centrifuged for 10 min at 3500 rpm, and left to equilibrate for 10 min at 25 °C to reach total phase separation and to ensure HSA and IgG depletion. After achieving the equilibrium conditions, the three phases were carefully separated. In almost all ABS, the aqueous phases were diluted and the interphase was resuspended in a phosphate buffer solution (PBS) for further analysis. The interphase of the ABS containing PPG 400 and the top phases of the ABS containing PE6200 and PE6400 were not analyzed due to solubilization issues. In these cases, the amount of IgG and HSA was calculated through mass balance to the initial amount added to each ABS. At least two replicas were prepared for each system, allowing to determine average values and the corresponding standard deviations. The amount of HSA and IgG in each phase was quantified by SE-HPLC using calibration curves previously established for IgG and HSA, both within the 0.1 – 1.0 mg·mL^{-1} range. The equipment used was a Chromaster HPLC system (VWR Hitachi) equipped with an analytical column (8 mm × 300 mm), Protein KW- 802.5, from Shodex, with a 50 mM sodium phosphate buffer and NaCl 0.3 M, run isocratically with a flow rate of 0.5 mL·min^{-1} during 40 min. The column oven and autosampler temperatures were kept at 25 °C and at 10 °C, respectively. The injection volume was of 25 µL and the wavelength was set at 280 nm, whereas the retention times of IgG and HSA were 15.21 min and 16.60 min, respectively.

The ABS performance to deplete IgG and HSA from commercial human serum by inducing their precipitation at the interphase was evaluated by their depletion efficiencies (DE_{IgG}, % and DE_{HSA}, %), according to the Equations 7 and 8:

$$DE_{IgG}, \% = \frac{w_{IgG}^{Inter}}{w_{IgG}^{Top} + w_{IgG}^{Inter} + w_{IgG}^{Bottom}} \times 100 \quad (7)$$

$$DE_{HSA}, \% = \frac{w_{HSA}^{Inter}}{w_{HSA}^{Top} + w_{HSA}^{Inter} + w_{HSA}^{Bottom}} \times 100 \quad (8)$$

where w_{IgG}^{Top}, w_{IgG}^{Inter} and w_{IgG}^{Bottom} represent, respectively, the weight of IgG in the top phase, in the interphase and in the bottom phase, and w_{HSA}^{Top}, w_{HSA}^{Inter}, w_{HSA}^{Bottom} represent the weight of HSA in the top phase, in the interphase and in the bottom phase, respectively.

2.4 Extraction of pentraxin 3

To evaluate the ABS-TPP ability to recover PTX-3, the systems containing PEG 1000, PEG 2000, PPG 400 and UCON were used. The same mixture composition as well as the protocol of ABS preparation and phases' separation as previously described was adopted with few adaptations. Instead of adding commercial human serum, an aqueous solution of PTX-3 (5 ng·mL^{-1}) or commercial human serum spiked with PTX-3 (at 5 ng·mL^{-1}) were introduced in the systems. The weight of PTX-3 on the aqueous phases of either the ABS or ABS-TPP, w_{PTX-3}^{Top} and w_{PTX-3}^{Bottom},was quantified using an ELISA kit following the manufacturer's instructions and using a calibration curve previously established (within the 15.6 - 1000 pg·mL^{-1} range). In turn, the weight of PTX-3 in the interphase of the ABS-TPP, w_{PTX-3}^{Inter}, was obtained through mass balance according to the Equation 9:

$$w_{PTX-3}^{Inter}\,(g) = w_{PTX-3}^{Initial} - w_{PTX-3}^{Top} - w_{PTX-3}^{Bottom} \quad (9)$$

where, $w_{PTX-3}^{Initial}$, w_{PTX-3}^{Top} and w_{PTX-3}^{Bottom} represent the weight of PTX-3 initially added in the ABS, and in the top and bottom phases, respectively.

The interference of the ABS components and proteins present in human serum samples within the quantification method was addressed through the implementation of blank controls (i.e., the same systems' compositions without PTX-3). At least three replicas of each system were employed, allowing to determine average values and the corresponding standard deviations.

The extraction efficiency of PTX-3 ($EE_{\mathrm{PTX\text{-}3}}$, %) towards the top phase was determined in the ABS comprising aqueous solutions of PTX-3 (and where no interphase is formed), according to the Equation 10:

$$EE_{PTX-3}, \% = \frac{w_{PTX-3}^{Top}}{w_{PTX-3}^{Top} + w_{PTX-3}^{Bottom}} \times 100 \quad (10)$$

where w_{PTX-3}^{Top} and w_{PTX-3}^{Bottom} are the total weight of PTX-3 in the top phase and in the bottom phase, respectively.

The recovery yields of PTX-3 ($RY_{\mathrm{PTX\text{-}3}}$, %) from human serum to the top, inter or bottom phases were calculated according to Equation 11:

$$RY_{PTX-3}, \% = \frac{w_{PTX-3}^{Top/Inter/Bottom}}{w_{PTX-3}^{Initial}} \times 100 \quad (11)$$

where $w_{PTX-3}^{Top/Inter/Bottom}$ is the total weight of PTX-3 in the top, inter or bottom phases and $w_{PTX-3}^{Initial}$ is the total weight of PTX-3 initially added in the spiked human serum.

To compare the accuracy of PTX-3 quantification obtained with and without pretreatment with the best performing ABS-TPP, the corresponding relative errors (*RE*, %) were determined according to the Equation 12:

$$RE, \% = \frac{w_{PTX-3}^{non-pretreated/ABS-TPP-pretreated} - w_{PTX-3}^{Initial}}{w_{PTX-3}^{Initial}} \times 100 \quad (12)$$

where $w_{PTX-3}^{non-pretreated/ABS-TPP-pretreated}$ is the total weight of PTX-3 in a non-pretreated spiked serum sample or in an ABS-TPP-pretreated sample (i.e., the top phase of the PEG 1000-based ABS-TPP) measured by ELISA, while $w_{PTX-3}^{Initial}$ is the exact weight of PTX-3 in the spiked serum (250 pg).

3. Results and discussion

In this work, ABS-TPP are proposed as a pretreatment step for human serum and PTX-3 extraction, while assisting quantification by ELISA. In ABS-TPP, it is envisaged that the high abundance proteins HSA and IgG are depleted through selective precipitation at the system interphase, while PTX-3 is fully extracted to the aqueous polymer-rich top phase. The used polymers were chosen because of the low cost, bio-friendliness, and capacity to act as protein precipitating agents [32,33]. Moreover, by varying the molecular weight as well as the monomeric composition/arrangement of the polymers, a wide range of hydrophobicity-hydrophilicity can be investigated, and more detailed structure-properties-performance relationships can be created to better design ABS-TPP as sample pretreatment and biomarker extraction techniques [34]. Citrate buffer ($K_3C_6H_5O_7/C_6H_8O$) at pH ≈ 7 was used as the common second component due to its salting-out effect and capacity to maintain the pH of the medium [35].

To develop ABS-TPP for human serum pretreatment, it is necessary to identify suitable ABS components and mixture compositions yielding two phases. To this aim, the cloud point titration method was used to determine the binodal curves of two groups of phase diagrams at 25 °C and atmospheric pressure [30], i.e., one composed of the homopolymers PPG 400 and PEGs 400, 600, 1000 and 2000, and other comprising the copolymers Pluronic PE6200, Pluronic PE6400, Pluronic L35 and UCON, both with citrate buffer ($K_3C_6H_5O_7/C_6H_8O_7$) at pH ≈ 7. All experimental binodal data is given in detail in the Supplementary Information (Table S1-S2). Compositions of homopolymer/copolymer and $K_3C_6H_5O_7/C_6H_8O_7$ above each binodal curve result in biphasic systems, whereas compositions below the same curve fit within the monophasic region. In systems with a larger biphasic region, the ability of both components to induce phase separation is higher, thus requiring lower amounts of polymer and $K_3C_6H_5O_7/C_6H_8O_7$ to form an ABS, as previously demonstrated [30]. In addition to the binodal curves, the characterization of the phase diagrams involved the estimation of the regression parameters (*A*, *B* and *C*) by the least-squares regression as well as the experimental tie-lines (TLs) and their corresponding lengths (TLLs). All related information can be found in the Supplementary Information (Table S3-S4) and is relevant due to the impact that both top and bottom phase compositions may have in the partition of proteins. It should be remarked that correlation coefficients (R^2) higher than 0.9766 were obtained, meaning that the correlation obtained can be used to predict the phase diagram behavior when no experimental data is available. In all systems, the top phase is polymer-rich, whereas the bottom phase is mainly constituted by $K_3C_6H_5O_7/C_6H_8O_7$. Despite all ABS being prepared at pH ≈ 7, the pH of both phases was also measured to control any deviation resultant from the polymers used that may influence the partition of the proteins (cf. Table S4 in the Supplementary Information).

Figure 2 shows the binodal curves in weight percent, enabling the direct identification of biphasic mixture compositions to be used in the development of the serum pretreatment step. Moreover, the relative position of the binodal curves provides information on the molecular-level mechanisms involved in the ABS formation and enables the establishment of an indirect polymer hydrophobicity scale [36,37]. Such information is useful to design/select more fit-for-purpose ABS components through the understanding of structure-properties-performance relationships. $K_3C_6H_5O_7/C_6H_8O_7$ is a strong salting-out species according to the Hofmeister series as it embodies a triply charged anion (i.e., $C_6H_5O_7^{3-}$) with strong hydration capacity [35]. Therefore, it presents a high affinity for water [38], being highly effective in the exclusion of the polymer from the aqueous solution, promoting the desired two-phase separation. Since the salt, temperature, pressure, and pH are constant, the ABS formation ability is both dependent on the type and molecular weight of the polymer.

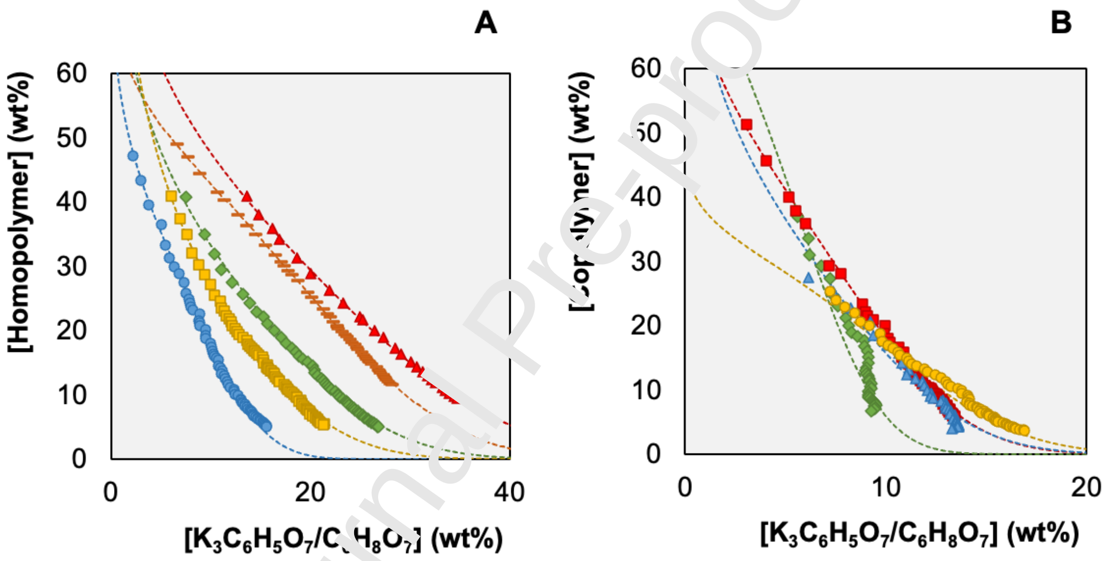

Figure 2. Binodal curves for the ABS composed of homopolymers (A) or copolymers (B) and $K_3C_6H_5O_7/C_6H_8O_7$ (pH ~ 7) at 25 °C and atmospheric pressure: (A) PEG 400 (red triangles), PEG 600 (orange rectangles), PEG 1000 (green diamonds), PEG 2000 (yellow squares), and PPG 400 (blue circle); (B) UCON (yellow circles), PE6400 (red squares), Pluronic L35 (blue triangles), and PE6200 (green diamonds). The dashed lines are the fitting of the experimental data obtained using the equation proposed by Merchuk et al. [31].

In what concerns the ability of homopolymers to induce liquid-liquid demixing, as shown in Figure 2A, the trend PPG 400 > PEG 2000 > PEG 1000 > PEG 600 > PEG 400 identifies PPG 400 as the most efficient polymer to form ABS in the presence of

$K_3C_6H_5O_7/C_6H_8O_7$. Overall, this trend complies with the molecular-level mechanisms reported in the literature as main drivers of polymer-salt ABS formation, where the salting out effect as well as the polymer molecular weight and hydrophobicity take a dominant part [39–41]. In brief, PPG is more hydrophobic than PEG due to the presence of an additional methyl group at the monomeric unit. It is thus possible to attribute to this structural feature the responsibility for the larger biphasic region observed with PPG 400 [42]. Regarding PEGs, a consecutive expansion of the two-phase region as the PEG molecular weight increases from 400 to 2000 $g{\cdot}mol^{-1}$ is observed. This trend derives from the increasing hydrophobicity of PEGs with higher molecular weights and their consequent lower water affinity, making them easier to be salted-out to the polymer-rich top phase by $K_3C_6H_5O_7/C_6H_8O_7$ [43].

For the copolymers (Figure 2B), the ranking Pluronic PE6200 > Pluronic L35 ≈ Pluronic PE6400 > UCON reflects two effects: (i) the percentage of PEG monomers in the copolymers composition (i.e., Pluronic PE 6200 versus Pluronic PE 6400); and (ii) the monomers arrangement in blocks or randomly in polymers with the same percentage of PEG (i.e., UCON versus Pluronic L35). First, Pluronic PE6200 is more easily salted out by $K_3C_6H_5O_7/C_6H_8O_7$ given its lower percentage of PEG monomers (20%), thus higher hydrophobic nature, than Pluronic PE6400 (40% of PEG monomers). Second, although it seems that Pluronic L35 has a higher ability to form ABS with $K_3C_6H_5O_7/C_6H_8O_7$ than the randomly arranged UCON, the differences observed in the binodal curves are small. Furthermore, the use of copolymers is advantageous since these may provide distinct behaviors as compared to their parent homopolymers and allow for a wider degree of structural versatility in ABS [44,45]. A reflection of this opportunity is disclosed by the relative position and shapes of the binodal curves of all ABS under investigation (cf. Figure 2), according to the following tendency (at [polymer] = [salt]): Pluronic PE6200 > Pluronic L35 ≈ Pluronic PE6400 ≈ PPG 400 > UCON > PEG 2000 > PEG 1000 > PEG 600 > PEG 400. In general, the ability of most copolymers to form ABS outpaces that of the homopolymers. Taking as reference PEG 2000 and Pluronics (that have similar molecular weights), the PPG content in the copolymers supports this behavior. Although PPG 400 is exclusively composed of more hydrophobic monomeric units, it has a lower molecular weight and its ability to form ABS is similar or even surpasses that of the copolymers.

Following the determination of the polymer-salt ABS that enabled the selection of a mixture point belonging to the biphasic region, ABS-TPP were formed by adding human serum [20]. A common mixture composition for all systems was adopted to appraise the depletion of high abundance serum proteins based on the binodal curves previously determined: 30 wt% of homopolymer/copolymer + 30 wt% of $K_3C_6H_5O_7/C_6H_8O_7$ + 5 wt% of human serum + 35 wt% of water. SE-HPLC was used to quantify IgG and HSA, allowing to determine the depletion efficiencies (DE_{IgG} and DE_{HSA}, %) shown in Figure 3. The Supplementary Information provides all details on the related data (Table S5).

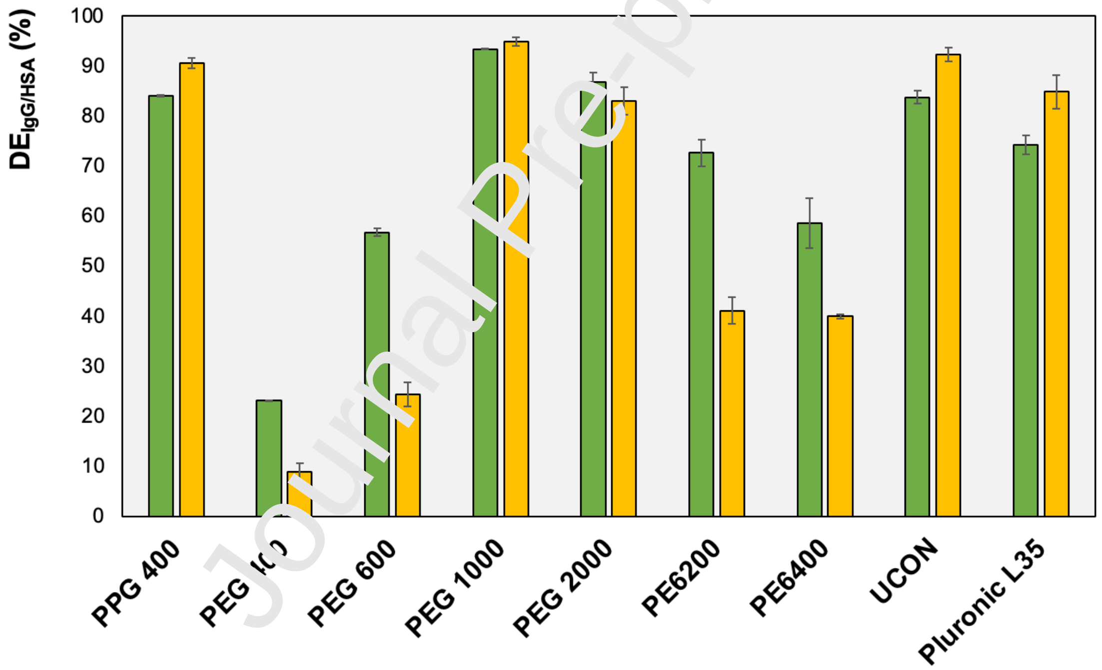

Figure 3. Depletion efficiencies of IgG (DE_{IgG}, %) (green bars) and HSA (DE_{HSA}, %) (yellow bars) obtained with ABS-TPP composed of 30 wt% of homopolymer/copolymer + 30 wt% of $K_3C_6H_5O_7/C_6H_8O_7$ + 5 wt% of human serum + 35 wt% of water.

The aptitude of the systems to deplete IgG agrees with the following sequence: PEG1000 > PEG 2000 > PPG 400 ≈ UCON > Pluronic L35 > Pluronic PE6200 > Pluronic PE6400 > PEG 600 > PEG 400. For HSA, the tendency changes according to the following ranking: PEG 1000 > UCON > PPG 400 > Pluronic L35 > PEG 2000 > Pluronic PE6200 > Pluronic PE6400 > PEG 600 > PEG 400. In the ABS-TPP studied, depletion efficiencies ranging between 23.2% and 93.4% for IgG and between 9% and 95% for HSA were obtained. Considering the data depicted in Figure 3, among the homopolymers studied, the ABS-TPP formed by PEG 1000 was the most efficient, followed by PEG 2000 and PPG 400. The lowest molecular weight (most hydrophilic) homopolymers (PEG 600 and PEG 400) achieved significantly lower depletion efficiencies of both proteins. Using copolymers, depletion efficiencies ranging from 59% to 84% for IgG and between 40% to 92% for HSA were achieved. The ABS-TPP formed by UCON yielded the highest depletion efficiencies for both HSA and IgG, followed by Pluronic L35, PE6200 and PE6400, as shown in Figure 3. It should be remarked that in all systems, the remaining proteins partitioned mainly to the polymer-rich top phase.

The partition and depletion of proteins in ABS-TPP are guided by several interactions established between the exposed groups of proteins and the phase-forming components [19,46,47]. The depletion of HSA and IgG at the interphase seems to be mainly driven by the combined action of the polymer, whose high concentration reduces the protein solubility in the polymer-rich top phase (cf. Table S4 in the Supplementary Information), and the salt capacity to bind to the proteins breaking intramolecular interactions [48–53]. To gather more insight on the role of the polymer hydrophobicity and further drawing structure-properties-performance relationships, a connection between the capacity of all polymers to undergo phase separation in the presence of $K_3C_6H_5O_7/C_6H_8O_7$ (i.e., polymer relative hydrophobicity) and the depletion efficiencies of both proteins can be generally established. Overall, ABS that are placed at relatively high to intermediate positions of the ABS formation ability trend, such as PEG 1000, PEG 2000, UCON and PPG 400, are more suitable to design the sample pretreatment technology allowing depletion efficiencies that are higher than 80% for both proteins. However, the influence of electrostatic interactions cannot be discarded because of the pH of the ABS-TPP (controlled at ≈7) and the proteins isoelectric points (pI) [54]. The pI of HSA and IgG are 4.7 and 6.5-9.5, respectively

[55,56]. Thus, regardless of the polymer, HSA is negatively charged (pH > pI) and IgG is electrically neutral (pH = pI). A more readily precipitation of proteins takes place at their pI due to reduced repulsive electrostatic forces that cause aggregation and precipitation [57]. In turn, negatively charged proteins are more soluble and not as susceptible to be precipitated [58]. Even negatively charged, almost all HSA precipitated at the interphase in the systems formed by PPG 400, PEG 1000, PEG 2000 and UCON (80+%). Although a significant portion of both HSA and IgG partitioned to the polymer-rich top phase in most remaining systems, electrostatic interactions do not seem to play a part: IgG is neutral and migrated preferentially to the polymer-rich top phase instead of precipitating as expected [59,60]. These results seem to exclude a significant effect of electrostatic interactions in the depletion of high abundance proteins in the systems and conditions under appraisal. Instead, the relevance of the polymer nature to design efficient serum pretreatment strategies resorting to ABS-TPP is reinforced [61,62].

Since our aim is to promote the depletion of high abundance proteins in the interphase, the significant partition of HSA and IgG to the polymer-rich top phase made the systems composed of PEG 600, PEG 400, Pluronic PE 6200 and Pluronic PE 6400 unsuitable for the target purpose. Thus, to evaluate the potential of ABS-TPP to simultaneously deplete HSA and IgG and completely extract PTX-3 from serum into an aqueous phase for further analysis by ELISA, ABS-TPP formed by the following polymers were investigated: PEG 1000, PEG 2000, PPG 400, UCON and Pluronic L35. Before studying human serum samples, ABS were initially prepared with an aqueous solution of PTX-3 at 5 $ng{\cdot}mL^{-1}$ – the cut-off value found in human serum for unhealthy donors [10] – to elucidate on the partition of this protein between the two phases using a simple matrix. Complete extraction (100%) of PTX-3 to the polymer-rich top phase was observed in all tested systems (Table S6 in the Supplementary Information).

After that, experiments with human serum spiked with PTX-3, at the same concentration as the previous tests, were conducted to evaluate the recovery yield of PTX-3 ($RY_{\text{PTX-3}}$, %) in each phase. These results are shown in Figure 4 and detailed in the Supplementary Information in Table S7, showing that the capacity of the polymers to extract PTX-3 from serum towards the polymer-rich top phase oblige to the following trend: PEG 1000 > UCON > Pluronic L35 > PEG 2000 > PPG 400.

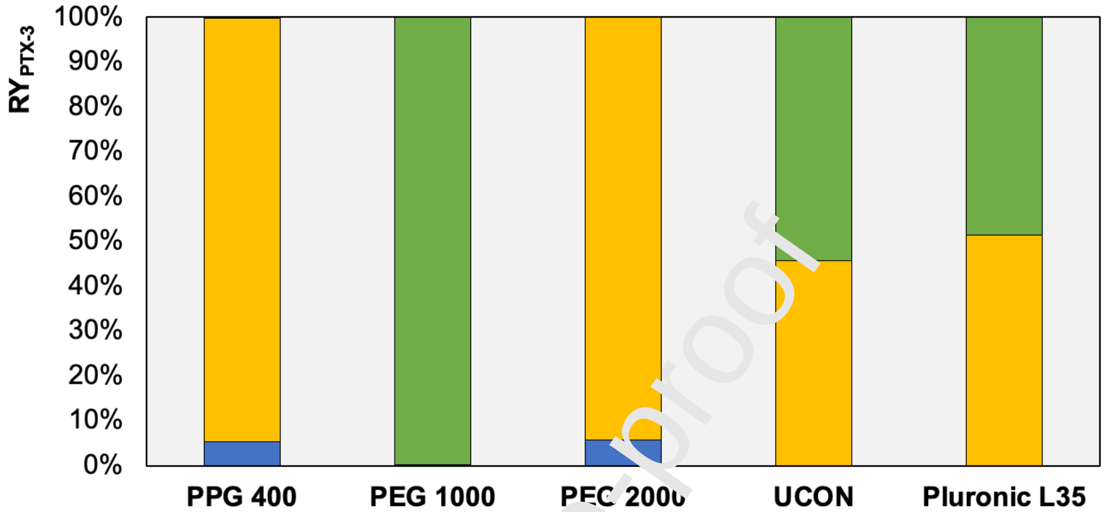

Figure 4. Recovery yields of PTX-3 (RY_{PTX-3}, %) for the top (green bars), inter (yellow bars), and bottom (blue bars) phases of the ABS-TPP composed of 30 wt% of homopolymer/copolymer + 30 wt% of $K_3C_6H_5O_7$/$C_6H_8O_7$ + 5 wt% of spiked human serum + 35 wt% water.

PTX-3 has a smaller size (≈45 KDa) than IgG (≈160 KDa) and HSA (≈66 KDa) and is also found in lower concentrations in human serum, being less prone to precipitate [63–65]. Furthermore, PTX-3 has a lower isoelectric point than the pH of the ABS (4.86 > 7), carrying negative charge [66]. Despite these properties, only the ABS formed by PEG 1000 allowed the complete extraction of PTX-3 (99.8%) from the spiked human serum to the polymer-rich top phase (Figure 4). Accordingly, PTX-3 is more soluble in the PEG 1000-rich phase and is not expected to precipitate at the interphase as significantly as IgG and HSA [67]. All remaining systems resulted in PTX-3 losses ranging from 46% to 94% to the interphase through the concomitant precipitation of PTX-3 and high abundance serum proteins. PPG 400, PEG 2000, UCON and Pluronic L35 rank higher on the ABS formation ability trend when compared to PEG 1000, indicating increased hydrophobicity. Like in the depletion of IgG and HSA, the higher hydrophobicity of the polymer, the lower the solubility of

PTX-3 in the polymer-rich phase, leading to precipitation at the interphase. The dependency of PTX-3 precipitation with the polymer molecular weight/hydrophobicity follows the general trends observed in the precipitation of proteins using polymers as precipitating agents [68]. Overall, the polymer's hydrophobic nature is the dominant factor behind the extraction/precipitation trends observed for PTX-3.

To further establish structure-properties-performance relationships, the capacity of all polymers to form ABS, depletion efficiencies of both HSA and IgG and recovery yields of PTX-3 to the polymer-rich top phase can be interlinked. If depletion of high abundance proteins is promoted by polymers of higher to intermediate hydrophobicity, a much narrower range of polymers structures/properties is suitable for the simultaneous depletion of HSA and IgG (>95%) and total extraction of PTX-3 (100%) to the polymer-rich top phase, as shown with PEG 1000.

Finally, the values of PTX-3 quantified by ELISA in the polymer-rich top phase following human serum pretreatment were compared with those quantified in a non-pretreated sample considering their percentage relative errors (*RE*, %). These results are shown in Table 1. Benchmarking the accuracy of PTX-3 analysis in serum by ELISA assisted by PEG 1000-based ABS-TPP against non-pretreated serum (spiked with PTX-3 at 5 $ng{\cdot}mL^{-1}$), a lower *RE*, i.e., 0.8 % versus 14.6%, in the PTX-3 quantification is accomplished following pretreatment with PEG 1000-based ABS-TPP. These results confirm the reduction of the interference of high abundance proteins within PTX-3 quantification, leading to more accurate results. Under the conditions used in this work, a polymer of intermediate molecular weight and hydrophobicity – PEG 1000 – was the only suitable option to develop efficient sample pretreatment strategies, while improving the accuracy of PTX-3 analysis by ELISA.

Table 1. Mass of PTX-3 quantified in an ABS-TPP-pretreated spiked sample and in a non-pretreated spiked sample, and their percentage relative errors (*RE*, %).

Human serum	w_{PTX-3} (pg)	*RE* (%)
ABS-TPP-pretreated sample	252.1 ± 4.7	0.8
Non-pretreated sample	287 ± 5	14.6

Based on the overall results, ABS are potential alternatives to the most used serum pretreatment techniques such as solid-phase extraction and protein precipitation, which fail to cumulatively provide high selectivity, high biomarker yield, enhanced practicality, and cost-efficiency [69–72]. In addition to the successful one-step depletion of high abundance serum proteins and biomarker extraction, our method provides simple and fast execution (serum samples are processed in ≈10 min in a single step), while using cheap and biocompatible constituents (PEG, water and $K_3C_6H_5O_7/C_6H_8O_7$) instead of high-cost protein ligand affinity or immunoaffinity resins as in some solid-phase extraction kits [73,74] or volatile organic solvents as adopted in some protein precipitation protocols [75].

We have recently shown that ionic liquids can be used to tailor the depletion of HSA and IgG from human serum using ABS [20]. By a proper design of the ionic liquid, such systems can improve the detection of a prostate cancer biomarker within microfluidic devices for point-of-care applications [76]. The current work enlarges the inventory of ABS-TPP to be used as serum pretreatment strategies by manipulating the homopolymer/copolymer molecular weight, arrangement, structure, and percentage of different monomers despite the narrow range of conditions enabling the simultaneous HSA/IgG depletion and PTX-3 extraction. It also demonstrates new opportunities for application, namely in clinical laboratory settings.

4. Conclusion

Herein we have proposed an accurate method to assess the levels of PTX-3 in human serum, while fostering its meaningfulness as a disease biomarker. The proposed method relies on ABS-TPP formed by PEG 1000 and $K_3C_6H_5O_7/C_6H_8O_7$ (pH ≈ 7) to assist quantification by ELISA. Our approach allows to simultaneously deplete high abundance serum proteins (depletion efficiencies >93% for HSA and IgG) and completely extract PTX-3 in the polymer-rich top phase, while improving the accuracy of analysis by ELISA. Overall, ABS-TPP may inspire the development of alternative pretreatment techniques for human samples and can be extended to other human samples as well as biomarkers of interest, bringing new prospects in clinical care to achieve more accurate diagnosis and prognosis.

CRediT authorship contribution statement

M.S.M.M.: Methodology, Validation, Formal analysis, Investigation, Data Curation, Writing-original draft, Visualization; M.E.R.: Methodology, Validation, Formal analysis, Investigation, Data Curation, Writing-original draft, Visualization; J.A.P.C.: Writing – review & editing, Supervision; M.G.F.: Conceptualization, Funding Acquisition, Supervision, Writing – review & editing; F.A.eS: Conceptualization, Writing – review & editing, Supervision, Funding Acquisition, Project Administration.

Declaration of Competing Interest

The authors declare that they have no known competing financial interests or personal relationships that could have appeared to influence the work reported in this paper.

Acknowledgments

This work was developed within the scope of the project CICECO-Aveiro Institute of Materials, UIDB/50011/2020, UIDP/50011/2020 & LA/P/0006/2020, financed by national funds through the FCT/MEC (PIDDAC). This work was developed within the project PTDC/EMD TLM/3253/2020 (ILSurvive), funded by national funds (OE), through FCT/MCTES. M.S.M.M. and M.E.R. acknowledge FCT for the doctoral grants 2022.11229.BD and SFRH/BD/136995/2018, respectively. F.A.eS. acknowledges FCT for the researcher contract CEECIND/03076/2018 under the Scientific Employment Stimulus – Individual Call 2018.

References

[1] A. Giacomini, G.C. Ghedini, M. Presta, R. Ronca, Long pentraxin 3: A novel multifaceted player in cancer, Biochim Biophys Acta Rev Cancer. 1869 (2018) 53–63. https://doi.org/10.1016/j.bbcan.2017.11.004.

[2] Z. Wang, X. Wang, H. Zou, Z. Dai, S. Feng, M. Zhang, G. Xiao, Z. Liu, Q. Cheng, The Basic Characteristics of the Pentraxin Family and Their Functions in Tumor

Progression, Front Immunol. 11 (2020) 1757. https://doi.org/10.3389/fimmu.2020.01757.

[3] L. Deban, B. Bottazzi, C. Garlanda, Y.M. de la Torre, A. Mantovani, Pentraxins: Multifunctional proteins at the interface of innate immunity and inflammation, BioFactors. 35 (2009) 138–145. https://doi.org/10.1002/biof.21.

[4] A. Mantovani, C. Garlanda, A. Doni, B. Bottazzi, Pentraxins in innate immunity: from C-reactive protein to the long pentraxin PTX3, J Clin Immunol. 28 (2008) 1–13. https://doi.org/10.1007/S10875-007-9126-7.

[5] C. Liu, Y. Yao, W. Wang, Pentraxin-3 as a prognostic marker in patients with small-cell lung cancer, Med Oncol. 31 (2014) 207. https://doi.org/10.1007/s12032-014-0207-1.

[6] F.C.G. de Aquino, T.M. Guedes, A. Pires, H.P. de Souza, Serum biomarkers for lung cancer screening, Rev Med (Rio J). 98 (2019) 59–71. https://doi.org/10.11606/issn.1679-9836.v98i1p60-72.

[7] C. Planque, V. Kulasingam, C.R. Smith, K. Reckamp, L. Goodglick, E.P. Diamandis, Identification of Five Candidate Lung Cancer Biomarkers by Proteomics Analysis of Conditioned Media of Four Lung Cancer Cell Lines, Mol Cell Proteomics. 8 (2009) 2746–2758. https://doi.org/10.1074/mcp.M900134-MCP200.

[8] S. Bhatnagar, D. Katare, S. Jain, Serum-based protein biomarkers for detection of lung cancer, Open Life Sci. 9 (2014) 341–358. https://doi.org/10.2478/s11535-013-0271-0.

[9] C. Garlanda, B. Bottazzi, E. Magrini, A. Inforzato, A. Mantovani, PTX3, a Humoral Pattern Recognition Molecule, in Innate Immunity, Tissue Repair, and Cancer, Physiol Rev. 98 (2018) 623–639. https://doi.org/10.1152/physrev.00016.2017.

[10] M. Infante, P. Allavena, C. Garlanda, M. Nebuloni, E. Morenghi, D. Rahal, M. Roncalli, S. Cavuto, S. Pesce, M. Monari, S. Valaperta, A. Montanelli, D. Solomon, E. Bottoni, V. Errico, E. Voulaz, M. Bossi, G. Chiesa, E. Passera, A. Mantovani, M. Alloisio, Prognostic and diagnostic potential of local and circulating levels of pentraxin 3 in lung cancer patients, Int J Cancer. 138 (2016) 983–991. https://doi.org/10.1002/IJC.29822.

[11] S. Liu, X. Qu, F. Liu, C. Wang, Pentraxin 3 as a Prognostic Biomarker in Patients with Systemic Inflammation or Infection, Mediators Inflamm. 2014 (2014) 1–9. https://doi.org/10.1155/2014/421429.

[12] M. Canovi, J. Lucchetti, M. Stravalaci, S. Valentino, B. Bottazzi, M. Salmona, A. Bastone, M. Gobbi, A New Surface Plasmon Resonance-Based Immunoassay for Rapid, Reproducible and Sensitive Quantification of Pentraxin-3 in Human Plasma, Sensors. 14 (2014) 10864–10875. https://doi.org/10.3390/s140610864.

[13] A.G. Paulovich, J.R. Whiteaker, A.N. Hoofnagle, P. Wang, The interface between biomarker discovery and clinical validation: The tar pit of the protein biomarker pipeline, Proteomics Clin Appl. 2 (2008) 1386–1402. https://doi.org/10.1002/PRCA.200780174.

[14] T. Waritani, J. Chang, B. McKinney, K. Terato, An ELISA protocol to improve the accuracy and reliability of serological antibody assays, MethodsX. 4 (2017) 153–165. https://doi.org/10.1016/J.MEX.2017.03.002.

[15] N.L. Anderson, N.G. Anderson, The Human Plasma Proteome: History, Character, and Diagnostic Prospects, Mol Cell Proteomics. 1 (2002) 845–867. https://doi.org/10.1074/MCP.R200007-MCP200.

[16] M. Karataş, S. Akgöl, H. Yavuz, R. Say, A. Denizli, Immunoglobulin G depletion from human serum with metal-chelated beads under magnetic field, Int J Biol Macromol. 40 (2007) 254–260. https://doi.org/10.1016/j.ijbiomac.2006.08.006.

[17] P.-Å. Albertsson, Partition of Proteins in Liquid Polymer–Polymer Two-Phase Systems, Nature. 182 (1958) 709–711. https://doi.org/10.1038/182709a0.

[18] M.C. Porfiri, G. Picó, D. Romanini, B. Farruggia, Aspergillus oryzae alpha-amylase partition in potassium phosphate-polyethylene glycol aqueous two-phase systems, Int J Biol Macromol. 49 (2011) 7–13. https://doi.org/10.1016/j.ijbiomac.2011.03.003.

[19] C. Shibata, K. Iwashita, K. Shiraki, Salt-containing aqueous two-phase system shows predictable partition of proteins with surface amino acids residues, Int J Biol Macromol. 133 (2019) 1182–1186. https://doi.org/10.1016/j.ijbiomac.2019.04.185.

[20] M. E. Rosa, M. S. M. Mendes, E. Carmo, J. P. Conde, J. A. P. Coutinho, M. G. Freire, F. A. e Silva, Tailored pretreatment of serum samples and biomarker extraction afforded by ionic liquids as constituents of aqueous biphasic systems, Sep Purif Technol. 322 (2023) 124248. https://doi.org/10.1016/j.seppur.2023.124248.

[21] E. Alvarez-Guerra, A. Irabien, Ionic liquid-based three phase partitioning (ILTPP) systems for whey protein recovery: ionic liquid selection, J Chem Technol Biotechol. 90 (2015) 939–946. https://doi.org/10.1002/jctb.4401.

[22] K. Hafid, J. John, T.M. Sayah, R. Domínguez, S. Becila, M. Lamri, A.L. Dib, J.M. Lorenzo, M. Gagaoua, One-step recovery of latex papain from Carica papaya using three phase partitioning and its use as milk-clotting and meat-tenderizing agent, Int J Biol Macromol. 146 (2020) 798–810. https://doi.org/10.1016/j.ijbiomac.2019.10.048.

[23] M.S.M. Mendes, M.E. Rosa, F. Ramalho, M.G. Freire, F.A. e Silva, Aqueous two-phase systems as multipurpose tools to improve biomarker analysis, Sep Purif Technol. 317 (2023) 123875. https://doi.org/10.1016/j.seppur.2023.123875.

[24] J. Schindler, U. Lewandrowski, A. Sickmann, E. Friauf, Aqueous polymer two-phase systems for the proteomic analysis of plasma membranes from minute brain samples, J Proteome Res. 5 (2006) 432–442. https://doi.org/10.1021/pr0704736.

[25] Y.H. Park, H.W. Shin, A.R. Jung, O.S. Kwon, Y.J. Choi, J. Park, J.Y. Lee, Prostate-specific extracellular vesicles as a novel biomarker in human prostate cancer, Sci Rep. 6 (2016) 1–9. https://doi.org/10.1038/srep30386.

[26] R. Hu, X. Feng, P. Chen, M. Fu, H. Chen, L. Guo, B.F. Liu, Rapid, highly efficient extraction and purification of membrane proteins using a microfluidic continuous-flow based aqueous two-phase system, J Chromatogr A. 1218 (2011) 171–177. https://doi.org/10.1016/j.chroma.2010.10.090.

[27] J.P. Frampton, J.B. White, A.B. Simon, M. Tsuei, S. Paczesny, S. Takayama, Aqueous two-phase system patterning of detection antibody solutions for cross-reaction-free multiplex ELISA, Sci Rep. 4 (2014) 14–16. https://doi.org/10.1038/srep04878.

[28] M.M. Pereira, J.D. Calixto, A.C.A. Sousa, B.J. Pereira, Á.S. Lima, J.A.P. Coutinho, M.G. Freire, Towards the differential diagnosis of prostate cancer by the pre-treatment of human urine using ionic liquids, Sci Rep. 10 (2020) 14931. https://doi.org/10.1038/s41598-020-71929-8.

[29] Y.H. Park, H.W. Shin, A.R. Jung, O.S. Kwon, Y.-J. Choi, J. Park, J.Y. Lee, Prostate-specific extracellular vesicles as a novel biomarker in human prostate cancer, Sci Rep. 6 (2016) 30386. https://doi.org/10.1038/srep30386.

[30] A.M. Ferreira, V.F.M. Faustino, D. Mondal, J.A.P. Coutinho, M.G. Freire, Improving the extraction and purification of immunoglobulin G by the use of ionic liquids as adjuvants in aqueous biphasic systems, J Biotechnol. 236 (2016) 166. https://doi.org/10.1016/J.JBIOTEC.2016.08.015.

[31] J.C. Merchuk, B.A. Andrews, J.A. Asenjo, Aqueous two-phase systems for protein separation: Studies on phase inversion, J Chromatogr B Biomed Sci Appl. 711 (1998) 285–293. https://doi.org/10.1016/S0378-4347(97)00594-X.

[32] N.F. Leininger, R. Clontz, J.L. Gainer, D.J. Kirwan, Polyethylene glycol-water and polypropylene glycol-water solutionsas benign reaction solvents, Chem Eng Commun. 190 (2010) 431–444. https://doi.org/10.1080/00986440302082.

[33] D. Matulis, Selective Precipitation of Proteins, Curr Protoc Protein Sci. 83 (2016). https://doi.org/10.1002/0471140864.ps0405s83.

[34] T. Reschke, C. Brandenbusch, G. Sadowski, Modeling aqueous two-phase systems: II. Inorganic salts and polyether homo- and copolymers as ATPS former, Fluid Phase Equilib. 375 (2014) 306–315. https://doi.org/10.1016/J.FLUID.2014.04.040.

[35] L.M. Pegram, M.T. Record, Hofmeister Salt Effects on Surface Tension Arise from Partitioning of Anions and Cations between Bulk Water and the Air−Water Interface, J Phys Chem B. 111 (2007) 5411–5417. https://doi.org/10.1021/jp070245z.

[36] A. Glyk, T. Scheper, S. Beutel, Influence of Different Phase-Forming Parameters on the Phase Diagram of Several PEG–Salt Aqueous Two-Phase Systems, J Chem Eng Data. 59 (2014) 850–859. https://doi.org/10.1021/je401002w.

[37] G. Tubío, L. Pellegrini, B.B. Nerli, G.A. Picó, Liquid−Liquid Equilibria of Aqueous Two-Phase Systems Containing Poly(ethylene glycols) of Different Molecular Weight and Sodium Citrate, J Chem Eng Data. 51 (2006) 209–212. https://doi.org/10.1021/je050332p.

[38] K.P. Ananthapadmanabhan, E.D. Goddard, Aqueous biphase formation in polyethylene oxide-inorganic salt systems, Langmuir. 3 (1987) 25–31. https://doi.org/10.1021/la00073a005.

[39] M.T. Zafarani-Moattar, S. Hamzehzadeh, S. Nasiri, A new aqueous biphasic system containing polypropylene glycol and a water-miscible ionic liquid, Biotechnol Prog. 28 (2012) 146–156. https://doi.org/10.1002/BTPR.718.

[40] P.G. Mazzola, A.M. Lopes, F.A. Hasmann, A.F. Jozala, T.C.V. Penna, P.O. Magalhaes, C.O. Rangel-Yagui, A. Pessoa, Liquid-liquid extraction of biomolecules: An overview and update of the main techniques, J Chemical Technol Biotechnol. 83 (2008) 143–157. https://doi.org/10.1002/JCTB.1794.

[41] B.A. Andrews, A.S. Schmidt, J.A. Asenjo, Correlation for the partition behavior of proteins in aqueous two-phase systems: Effect of surface hydrophobicity and charge, Biotechnol Bioeng. 90 (2005) 380–390. https://doi.org/10.1002/BIT.20495.

[42] H. Mohamed, S. Hudziak, V. Arumuganathan, Z. Meng, M.-O. Coppens, Effects of charge and hydrophilicity on the anti-fouling properties of kidney-inspired, polyester membranes, Mol Syst Des Eng. 5 (2020) 1219–1229. https://doi.org/10.1039/D0ME00045K.

[43] R.M. De Oliveira, J.S. Dos Reis Coimbra, L.A. Minim, L.H.M. Da Silva, M.P.F. Fontes, Liquid–Liquid Equilibria of Biphasic Systems Composed of Sodium Citrate + Polyethylene(glycol) 1500 or 4000 at Different Temperatures, J Chem Eng Data. 53 (2008) 895–899. https://doi.org/10.1021/JE7004209.

[44] F.G. Ahsaie, G. Pazuki, T.E. Sintra, P. Carvalho, S.P.M. Ventura, Study of the partition of sodium diclofenac and norfloxacin in aqueous two-phase systems based on copolymers and dextran, Fluid Phase Equilib. 530 (2021) 112868. https://doi.org/10.1016/J.FLUID.2020.112868.

[45] M.C. de Oliveira, M.A.N. de Abreu Filho, P. de A. Pessôa Filho, Phase equilibrium and protein partitioning in aqueous two-phase systems containing ammonium carbamate and block copolymers PEO–PPO–PEO, Biochem Eng J. 37 (2007) 311–318. https://doi.org/10.1016/J.BEJ.2007.05.010.

[46] C.K. Su, B.H. Chiang, Partitioning and purification of lysozyme from chicken egg white using aqueous two-phase system, Process Biochem. 41 (2006) 257–263. https://doi.org/10.1016/J.PROCBIO.2005.06.026.

[47] M.V. Rocha, B.B. Nerli, Molecular features determining different partitioning patterns of papain and bromelain in aqueous two-phase systems, Int J Biol Macromol. 61 (2013) 204–211. https://doi.org/10.1016/j.ijbiomac.2013.06.055.

[48] M. Fahie-Wilson, D. Halsall, Polyethylene glycol precipitation: proceed with care, Ann Clin Biochem. 45 (2008) 233–235. https://doi.org/10.1258/ACB.2008.007262.

[49] S. Großhans, G. Wang, J. Hubbuch, Water on hydrophobic surfaces: mechanistic modeling of polyethylene glycol-induced protein precipitation, Bioprocess Biosyst Eng. 42 (2019) 513–520. https://doi.org/10.1007/s00449-018-2054-5.

[50] N. Samanta, T.Q. Luong, D. Das Mahanta, R.K. Mitra, M. Havenith, Effect of Short Chain Poly(ethylene glycol)s on the Hydration Structure and Dynamics around Human Serum Albumin, Langmuir. 32 (2016) 831–837. https://doi.org/10.1021/acs.langmuir.5b03884.

[51] J.A. Asenjo, B.A. Andrews, Aqueous two-phase systems for protein separation: A perspective, J Chromatogr A. 1218 (2011) 8826–8835. https://doi.org/10.1016/J.CHROMA.2011.06.051.

[52] S. Kalaivani, I. Regupathi, Partitioning studies of α-lactalbumin in environmental friendly poly (ethylene glycol)--citrate salt aqueous two phase systems, Bioprocess Biosyst Eng. 36 (2013) 1475–1483. https://doi.org/10.1007/S00449-013-0910-X.

[53] R. Iyyaswami, P.D. Belur, B. Girish, V.H. Nagaraj, Development and Evaluation of PEG-Lithium Citrate Salt Based Aqueous Two Phase System and Its Application in Partitioning of Proteins from Fish Industry Effluent, Sep Sci Technol. 47 (2012) 591–598. https://doi.org/10.1080/01496395.2011.626009.

[54] B.B. Nerli, M. Espariz, G.A. Picó, Thermodynamic study of forces involved in bovine serum albumin and ovalbumin partitioning in aqueous two-phase systems, Biotechnol Bioeng. 72 (2001) 468–474. https://doi.org/10.1002/1097-0290(20000220)72:4<468::AID-BIT1008>3.0.CO;2-L.

[55] I.M. Vlasova, A.M. Saletsky, Study of the denaturation of human serum albumin by sodium dodecyl sulfate using the intrinsic fluorescence of albumin, J Appl Spectrosc. 76 (2009) 536–541. https://doi.org/10.1007/s10812-009-9227-6.

[56] F. Chiodi, Å. Sidén, E. Ösby, Isoelectric focusing of monoclonal immunoglobulin G, A and M followed by detection with the avidin-biotin system, Electrophoresis. 6 (1985) 124–128. https://doi.org/10.1002/elps.1150060305.

[57] C. Dennison, R. Lovrien, Three Phase Partitioning: Concentration and Purification of Proteins, Protein Expr Purif. 11 (1997) 149–161. https://doi.org/10.1006/prep.1997.0779.

[58] R.M. Kramer, V.R. Shende, N. Motl, C.N. Pace, J.M. Scholtz, Toward a Molecular Understanding of Protein Solubility: Increased Negative Surface Charge Correlates with Increased Solubility, Biophys J. 102 (2012) 1907–1915. https://doi.org/10.1016/j.bpj.2012.01.060.

[59] A.M. Azevedo, P.A.J. Rosa, I.F. Ferreira, M.R. Aires-Barros, Optimisation of aqueous two-phase extraction of human antibodies, J Biotechnol. 132 (2007) 209–217. https://doi.org/10.1016/j.jbiotec.2007.04.002.

[60] A.M. Azevedo, A.G. Gomes, P.A.J. Rosa, I.F. Ferreira, A.M.M.O. Pisco, M.R. Aires-Barros, Partitioning of human antibodies in polyethylene glycol–sodium citrate aqueous two-phase systems, Sep Purif Technol. 65 (2009) 14–21. https://doi.org/10.1016/j.seppur.2007.12.010.

[61] F. Qu, H. Qin, M. Dong, D.X. Zhao, X.Y. Zhao, J.H. Zhang, Selective separation and enrichment of proteins in aqueous two-phase extraction system, Chin Chem Lett. 20 (2009) 1100–1102. https://doi.org/10.1016/j.cclet.2009.04.023.

[62] A.R. Salabat, M.H. Abnosi, A. Motahari, Application of aqueous mixtures of polypropylene glycol or polyethylene glycol with salts in proteomic analysis, J Iran Chem Soc. 7 (2010) 142–149. https://doi.org/10.1007/BF03245871.

[63] S. Bastrup-Birk, M.-O. Skjoedt, L. Munthe-Fog, J.J. Strom, Y.J. Ma, P. Garred, Pentraxin-3 Serum Levels Are Associated with Disease Severity and Mortality in Patients with Systemic Inflammatory Response Syndrome, PLoS One. 8 (2013) e73119. https://doi.org/10.1371/journal.pone.0073119.

[64] D. Prozeller, C. Rosenauer, S. Morsbach, K. Landfester, Immunoglobulins on the surface of differently charged polymer nanoparticles, Biointerphases. 15 (2020) 031009. https://doi.org/10.1116/6.0000139.

[65] R. Raoufinia, A. Mota, N. Keyhanvar, F. Safari, S. Shamekhi, J. Abdolalizadeh, Overview of Albumin and Its Purification Methods, Adv Pharm Bull. 6 (2016) 495–507. https://doi.org/10.15171/apb.2016.063.

[66] V. Rivieccio, A. Esposito, P. Bellofiore, P. Palladino, M. Sassano, M. Colombo, A. Verdoliva, High-level expression and efficient purification of recombinant human long

pentraxin PTX3 in Chinese hamster ovary cells, Protein Expr Purif. 51 (2007) 49–58. https://doi.org/10.1016/j.pep.2006.07.009.

[67] R.N. Pereira, R.M. Rodrigues, Ó.L. Ramos, F. Xavier Malcata, J.A. Teixeira, A.A. Vicente, Production of Whey Protein-Based Aggregates Under Ohmic Heating, Food Bioproc Tech. 9 (2016) 576–587. https://doi.org/10.1007/s11947-015-1651-4.

[68] A. Polson, G.M. Potgieter, J.F. Largier, G.E.F. Mears, F.J. Joubert, The fractionation of protein mixtures by linear polymers of high molecular weight, Biochim Biophys Acta - Gen Subj. 82 (1964) 463–475. https://doi.org/10.1016/0304-4165(64)90438-6.

[69] Z. Ning, B. Hawley, D. Seebun, D. Figeys, APols-Aided Protein Precipitation: A Rapid Method for Concentrating Proteins for Proteomic Analysis, J Membr Biol. 247 (2014) 941–947. https://doi.org/10.1007/s00232-014-9668-6.

[70] P.Y. Lee, J. Osman, T.Y. Low, R. Jamal, Plasma/serum proteomics: Depletion strategies for reducing high-abundance proteins for biomarker discovery, Bioanalysis. 11 (2019) 1799–1812. https://doi.org/10.4155/bio-2019-0145.

[71] C. Bylda, R. Thiele, U. Kobold, D.A. Volmer, Recent advances in sample preparation techniques to overcome difficulties encountered during quantitative analysis of small molecules from biofluids using LC-MS/MS, Analyst. 139 (2014) 2265–2276. https://doi.org/10.1039/c4an00094c.

[72] Y.-Y. Chen, S.-Y. Lin, Y.-Y. Yeh, H.-H. Hsiao, C.-Y. Wu, S.-T. Chen, A.H.-J. Wang, A modified protein precipitation procedure for efficient removal of albumin from serum, Electrophoresis. 26 (2005) 2117–2127. https://doi.org/10.1002/elps.200410381.

[73] Sigma-Aldrich, ProteoPrep® Immunoaffinity Albumin & IgG Depletion Kit, (2023). https://www.sigmaaldrich.com/PT/en/product/sigma/protia?gclid=Cj0KCQjwsp6pBhCfARIsAD3GZua_tLNEY60HP7cqaoDxXkiQo4FZu5GfIIykxQxsumiqIaxV0dZ2KgYaAtjuEALw_wcB (accessed October 12, 2023).

[74] Sigma-Aldrich, HiTrap® Albumin IgG Depletion, (2023). https://www.sigmaaldrich.com/PT/en/product/sigma/ge28946603?gclid=Cj0KCQjwsp6pBhCfARIsAD3GZuZ7sQlCmCja1Ux850zE7qXBY3jhTQh4D3s47y9Qa-Y1nFDs7EXjIQIaAkCEEALw_wcB (accessed October 12, 2023).

[75] T.M. Alshammari, A.A. Al-Hassan, T.B. Hadda, M. Aljofan, Comparison of different serum sample extraction methods and their suitability for mass spectrometry analysis, Saudi Pharm J. 23 (2015) 689–697. https://doi.org/10.1016/j.jsps.2015.01.023.

[76] F.C. Flora, S.B. Relvas, F.A. e Silva, M.G. Freire, V. Chu, J.P. Conde, Combined Use of Ionic Liquid-Based Aqueous Biphasic Systems and Microfluidic Devices for the Detection of Prostate-Specific Antigen, Biosensors. 13 (2023) 334. https://doi.org/10.3390/bios13030334.

Highlights

- ABS are used to deplete HSA and IgG and extract PTX-3 prior to analysis by ELISA.
- ABS are formed by combining citrate buffer with homopolymers/copolymers.
- Both HSA/IgG depletion and PTX-3 extraction depend on the polymers' properties.
- PEG 1000 enables 93+% depletion of HSA/IgG and 100% extraction of PTX-3 from serum.
- Higher accuracy in serum PTX-3 quantification is enabled after the ABS pretreatment.